Article

Cancer Cell

Co-inhibition of CD73 and A2AR Adenosine Signaling Improves Anti-tumor Immune Responses

Graphical Abstract

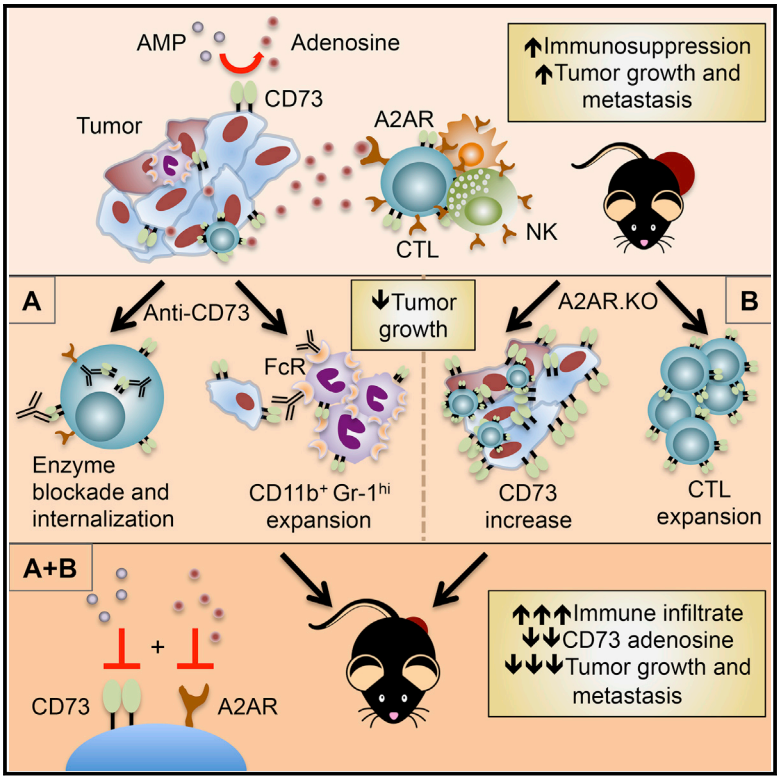

Highlights

- Functions of CD73 and A2AR are not redundant within the tumor microenvironment
- Co-targeting CD73 and A2AR reduced tumor initiation, growth, and metastasis
- Anti-CD73 requires Fc receptor engagement for optimal therapeutic response in mice

Authors

Arabella Young, Shin Foong Ngiow, Deborah S. Barkauskas, ..., Michele W.L. Teng, Kris Sachsenmeier, Mark J. Smyth

Correspondence

mark.smyth@qimrberghofer.edu.au

In Brief

Young et al. show that blockade of CD73 and A2AR, two components of the adenosinergic pathway, has more potent anti-tumor activity than blockade of either, partly due to increased CD73 expression in the absence of A2AR. Moreover, anti-CD73 antibodies require the FcR binding domain for optimal anti-tumor activity.

Young et al., 2016, Cancer Cell *30*, 391–403
September 12, 2016
http://dx.doi.org/10.1016/j.ccell.2016.06.025

Cancer Cell
Article

Co-inhibition of CD73 and A2AR Adenosine Signaling Improves Anti-tumor Immune Responses

Arabella Young,[1,2] Shin Foong Ngiow,[1,2] Deborah S. Barkauskas,[1] Erin Sult,[3] Carl Hay,[3] Stephen J. Blake,[4] Qihui Huang,[3] Jing Liu,[1,2,4] Kazuyoshi Takeda,[5] Michele W.L. Teng,[2,4] Kris Sachsenmeier,[3] and Mark J. Smyth[1,2,6,*]
[1]Immunology in Cancer and Infection Laboratory, QIMR Berghofer Medical Research Institute, 300 Herston Road, Herston, QLD 4006, Australia
[2]School of Medicine, The University of Queensland, Herston, QLD 4006, Australia
[3]MedImmune, LLC., Gaithersburg, MD 20878, USA
[4]Cancer Immunoregulation and Immunotherapy, QIMR Berghofer Medical Research Institute, Herston, QLD 4006, Australia
[5]Division of Cell Biology, Biomedical Research Center, Graduate School of Medicine, Juntendo University, Bunkyo-ku, Tokyo 113-8421, Japan
[6]Lead Contact
*Correspondence: mark.smyth@qimrberghofer.edu.au
http://dx.doi.org/10.1016/j.ccell.2016.06.025

SUMMARY

Preclinical studies targeting the adenosinergic pathway have gained much attention for their clinical potential in overcoming tumor-induced immunosuppression. Here, we have identified that co-blockade of the ectonucleotidase that generates adenosine CD73 and the A2A adenosine receptor (A2AR) that mediates adenosine signaling in leuokocytes, by using compound gene-targeted mice or therapeutics that target these molecules, limits tumor initiation, growth, and metastasis. This tumor control requires effector lymphocytes and interferon-γ, while antibodies targeting CD73 promote an optimal therapeutic response in vivo when engaging activating Fc receptors. In a two-way mixed leukocyte reaction using a fully human anti-CD73, we demonstrated that Fc receptor binding augmented the production of proinflammatory cytokines.

INTRODUCTION

Adenosine is a potent immunosuppressor, essential in maintaining tissue homeostasis and preventing an overzealous immune response during inflammation and infection (Ohta and Sitkovsky, 2001). However, within the tumor microenvironment (TME) adenosine hampers the immune reaction toward cancer cells. In particular, adenosine disables the cytotoxic anti-tumor immune response, while enhancing the proliferation and polarization of immunosuppressive cells and the neovascularization that supports tumor growth (Young et al., 2014). Therefore, modulating adenosine levels in the TME may limit tumor growth and improve anti-tumor immune activity. Both inhibition of adenosine generation and signaling have been shown to be effective therapeutic approaches (Beavis et al., 2013; Ohta et al., 2006; Stagg et al., 2010). Hypoxia heightens adenosine production, and when ablated significantly reduced tumor burden via an A2A adenosine receptor (A2AR)-dependent mechanism (Hatfield et al., 2014, 2015). Importantly, decreasing tumor-derived extracellular adenosine by respiratory hyperoxia improved the cytotoxic capacity of $CD8^+$ T and natural killer (NK) cells (Hatfield et al., 2014). These studies and others (reviewed in Young et al., 2014) illustrated the therapeutic potential of targeting the adenosinergic pathway in cancer.

Antibody-mediated immune checkpoint blockade against programmed death 1 (PD-1) and cytotoxic T lymphocyte associated 4 (CTLA-4) have generated durable responses in cancer patients (Ott et al., 2013; Smyth et al., 2015). However, some patients are non-responsive to this class of therapy, indicating that alternative immunosuppressive mechanisms must be targeted in

Significance

Single adenosine-related therapies have demonstrated anti-tumor efficacy in preclinical mouse models. Despite being formidable alternatives or partners to immune checkpoint antibodies in relieving tumor-induced immunosuppression, adenosine-related therapies are only now entering early-phase clinical trials in cancer. While it would seem likely that approaches targeting CD73, the ectonucleotidase that generates extracellular adenosine, and A2AR, the high-affinity receptor for adenosine on immune cells, might be redundant, intriguingly we show this is not the case. Co-blockade of CD73 and A2AR demonstrates that targeting multiple points of the adenosinergic pathway may be of significant therapeutic benefit. In interrogating this mechanism using mouse models we also discover that FcR binding domains of anti-CD73 antibodies enhance therapeutic response.

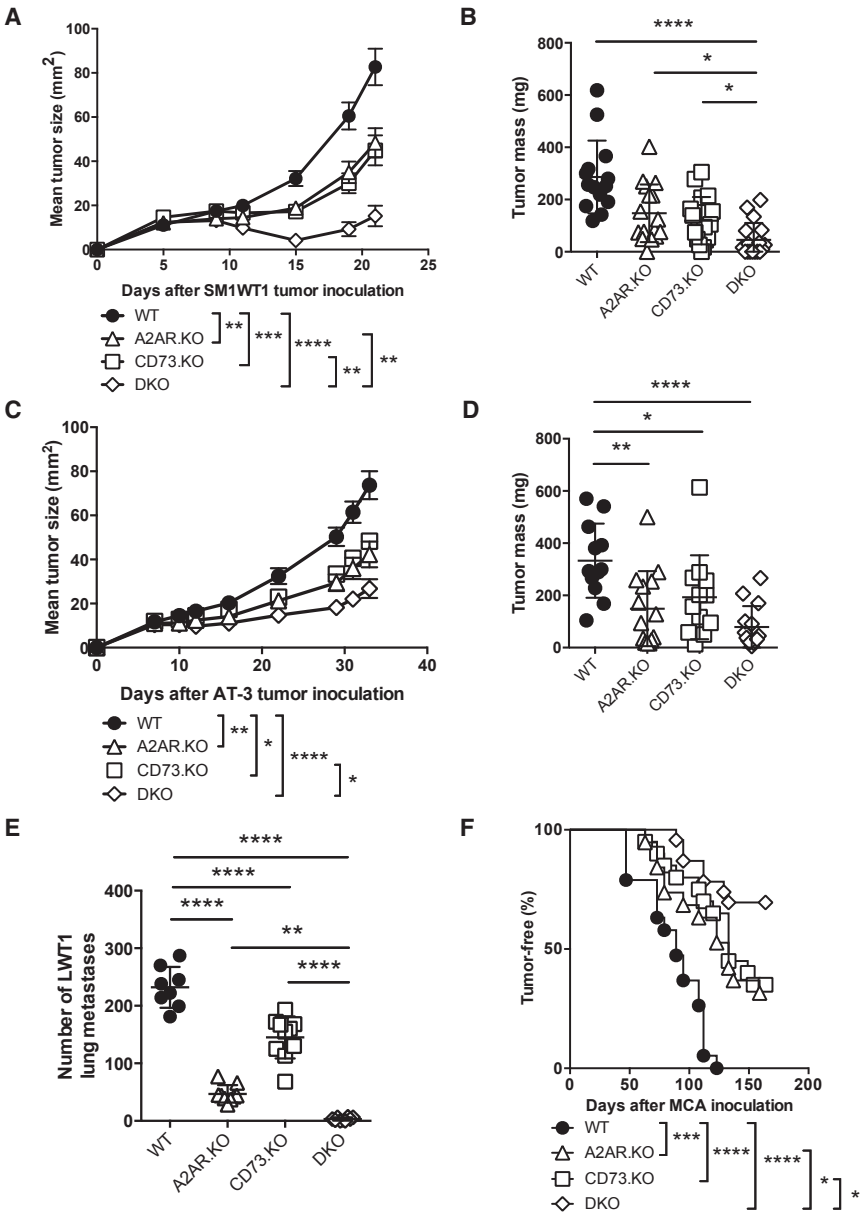

Figure 1. Co-targeting Host A2AR and CD73 Improves Anti-tumor Efficacy

(A) Growth of subcutaneous SM1WT1 tumor in C57BL/6 WT, A2AR.KO, CD73.KO, and DKO mice, with tumor sizes presented as mean ± SEM and statistical significance determined on day 21.

(B) SM1WT1 tumors as in (A) were excised on day 22, and tumor mass measured and presented as mean ± SD.

(C) Growth of subcutaneous AT-3 tumors in WT or indicated gene-targeted mice, with tumor sizes presented as mean ± SEM and statistical significance determined on day 33.

(D) AT-3 tumors as in (C) were excised on day 36, and tumor mass measured and presented as mean ± SD.

(E) Numbers of macrometastases in lung (mean ± SD) of WT or gene-targeted mice on day 14 after being inoculated intravenously with LWT1.

(F) Percentage of tumor-free WT or gene-targeted mice following inoculation with MCA. *$p < 0.05$, ***$p < 0.001$, ****$p < 0.0001$ determined by log-rank (Mantel-Cox) test.

In (A–E) results are pooled from two experiments and 12–17 mice per group (A–D) or from one experiment and eight to ten mice per group (E). *$p < 0.05$, **$p < 0.01$, ***$p < 0.001$, ****$p < 0.0001$ determined by one-way ANOVA and Holm-Sidak multiple comparison test between indicated pairwise combinations. See also Figures S1 and S2.

combination to provide maximal therapeutic benefit (Teng et al., 2015). Interestingly, blockade of adenosine generation via CD73 and signaling via the A2AR (predominantly expressed on immune cells) increases the therapeutic efficacy of clinically approved immunotherapies in preclinical models (Allard et al., 2013; Beavis et al., 2015; Iannone et al., 2014; Mittal et al., 2014). This suggests the possible benefits of utilizing adenosine-related therapeutic approaches in combination with current clinically approved immunomodulators.

While antagonists of A2AR signaling are undergoing clinical testing for the treatment of Parkinson's disease and display excellent safety profiles, their redeployment into oncology is only just occurring. Recently, recruitment has commenced for a clinical trial to identify the possible benefits of anti-CD73 antibody treatment alone and in combination with anti-PD-L1 antibody for solid tumors (NCT02503774). However, it is yet to be established whether targeting multiple points of the adenosinergic pathway in combination may further enhance anti-tumor efficacy.

RESULTS

A2AR and CD73 Double-Deficient Mice Display Enhanced Tumor Control

To determine whether limiting the generation of adenosine and adenosine signaling in the TME is redundant, we developed gene-targeted mice deficient for both the A2AR and CD73 (herein referred to as DKO). These mice displayed baseline immune repertoires similar to those of syngeneic wild-type (WT) and single-gene-deficient mice in both spleen and peripheral blood (Figure S1). We initiated our studies using transplantable AT-3 mammary carcinoma and SM1WT1 BRAF-mutated melanoma tumor models, which had previously been determined to be anti-PD-1 resistant (Knight et al., 2013; Ngiow et al., 2015). These tumor cell lines expressed low levels of CD73 in vitro (Figures S2A and S2B). SM1WT1 subcutaneous tumors were significantly reduced in size and mass in DKO mice in comparison with A2AR.KO, CD73.KO, and WT mice (Figures 1A, 1B, and S2C). In addition, more than 40% of DKO mice challenged with SM1WT1 rejected their tumors compared with less than 7% of the single-gene-targeted counterparts (Figure S2C). Similar results were seen in the AT-3 tumor model, in which the

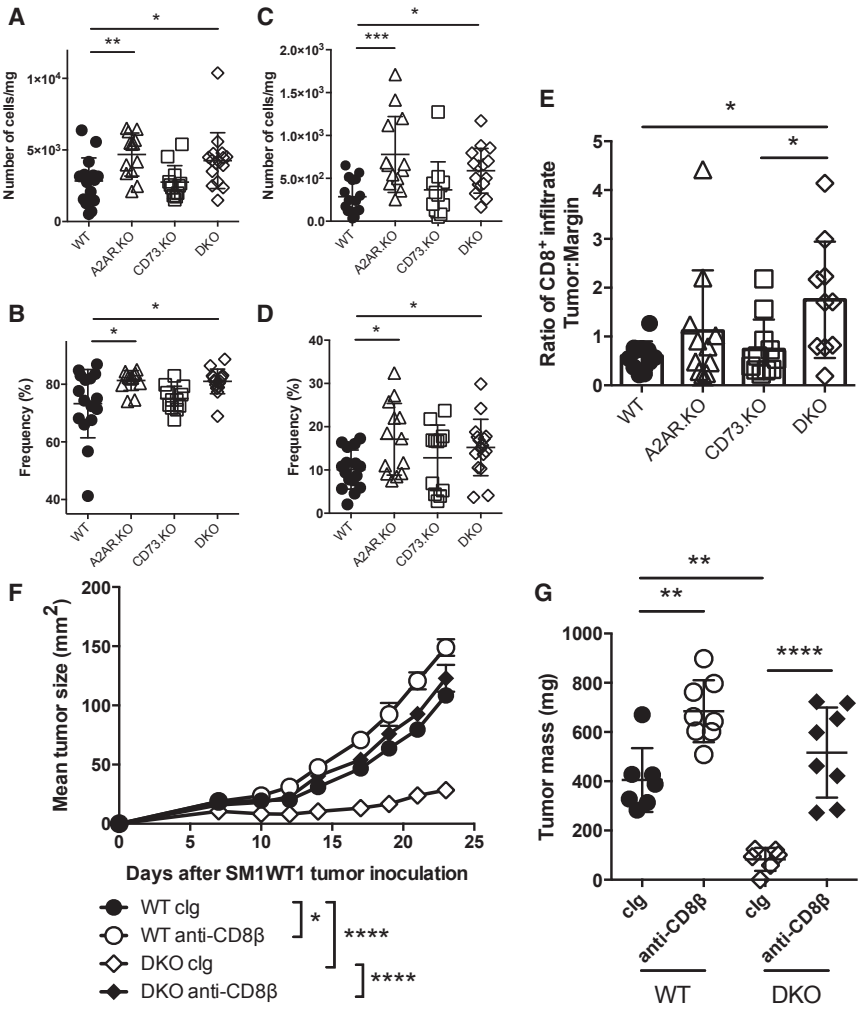

Figure 2. A2AR-Deficient Mice Display Improved CD8$^+$ T Cell Infiltration into the Tumor

(A and B) Number (A), normalized to tumor mass, and proportions (B) of live lymphocytes (gated on CD45.2$^+$, 7AAD$^-$) in SM1WT1 tumors grown in indicated mice harvested at day 8.

(C and D) Number (C), normalized to tumor mass, and proportions (D) of CD8$^+$ T cell in day 8 SM1WT1 tumors grown in indicated mice.

(E) Ratio of CD8$^+$ infiltrate within the tumor core versus the margin of day 8 SM1WT1 tumors was assessed via immunofluorescence.

(F) SM1WT1 tumor growth in WT and DKO mice depleted of CD8$^+$ T cells by treatment with anti-CD8β (100 μg intraperitoneally) on days −1, 0, 7, 14, and 21. Tumor sizes are presented as mean ± SEM and statistical significance was determined on day 23.

(G) Mass of SM1WT1 tumors as in (F) excised on day 24.

Results are presented as mean ± SD unless indicated otherwise from two pooled experiments of groups of 12–16 mice (A–D) or 10–11 mice per group (E), or from one experiment of seven to eight mice per group (F and G). *$p < 0.05$, **$p < 0.01$, ***$p < 0.001$, ****$p < 0.0001$ determined by one-way ANOVA and Holm-Sidak multiple comparison test between indicated pairs.

See also Figure S3.

DKO mice displayed significantly greater reduction in tumor burden compared with WT mice than the single-gene-targeted mice (Figures 1C, 1D, S2D, and S2E).

We next assessed whether DKO mice could limit metastatic formation. Using the experimental metastatic melanoma LWT1 derived from SM1WT1 (Ferrari de Andrade et al., 2014), we identified that single-gene-targeted mice displayed improved metastatic control compared with WT mice, which was further enhanced in DKO mice (Figure 1E). We also assessed the survival of DKO and control mice intravenously inoculated with RMA-s lymphoma cells, which lack major histocompatibility complex class I expression and are controlled by NK cells (Swann et al., 2007). The DKO mice had better survival than WT and single-gene-targeted control strains (Figure S2F).

To further substantiate the effects of co-targeting A2AR and CD73 in a de novo model of primary tumor formation, we utilized the methylcholanthrene (MCA)-induced fibrosarcoma model. Using this model, loss of host A2AR or CD73 has been previously shown to significantly decrease tumor initiation and enhance survival (Eini et al., 2015; Stagg et al., 2012). Consistent with these findings A2AR.KO and CD73.KO mice displayed significantly delayed tumor development compared with WT mice (Figure 1F). Interestingly, the DKO mice displayed a significantly lower incidence of tumor initiation in comparison with both A2AR and CD73 single-deficient strains (Figure 1F).

Collectively, these data showed that targeting A2AR and CD73 together reduced tumor initiation, growth, and dissemination. This is indicative that A2AR and CD73 possess distinct roles in tumor development and progression.

A2AR-Deficient Mice Display Improved Lymphocyte Infiltration into the Tumor

Next, we assessed the mechanism by which co-deletion of A2AR and CD73 enhanced anti-tumor efficacy. Since adenosine is a notable immunosuppressive metabolite (Young et al., 2014), we first interrogated the tumor-infiltrating leukocytes (TILs). Analysis of SM1WT1 primary tumors at day 8 was performed since TILs could be obtained and there was no significant difference in the mean tumor size observed in various host strains. SM1WT1 tumors harvested from mice that lacked A2AR signaling (both A2AR.KO and DKO) displayed increased proportions and numbers of TILs compared with WT mice (Figures 2A and 2B). Specifically, the A2AR-deficient mice displayed significantly increased intratumor CD8$^+$ T cell frequency and number (Figures 2C and 2D). No other immune cell populations that were assessed (CD4$^+$ T, NK, and myeloid cells) displayed significant changes in both their frequency and number upon loss of A2AR and/or CD73 (Figure S3A).

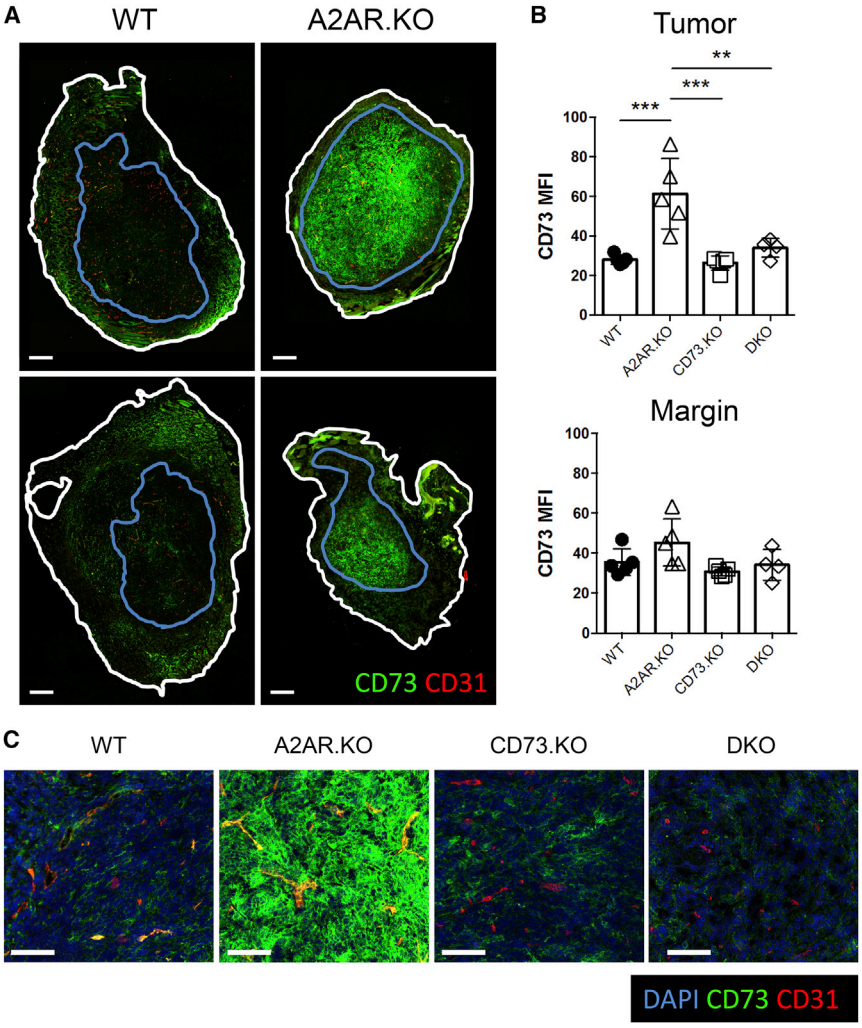

Figure 3. CD73 Expression Is Increased within the Tumor Core of A2AR-Deficient Mice

(A) Representative images of sections of fresh-frozen day 8 SM1WT1 tumors grown in WT or A2AR.KO mice stained for CD73 and CD31. Tumor sections are divided into tumor core (inside the blue line) and invasive margin (between the blue and white line) based on the intensity of DAPI staining (not shown). Scale bars represent 200 μm. (B) CD73 MFI in the tumor core and margin of tumor as in (A) was determined and presented as mean ± SD from one representative experiment of four to five mice from the indicated genotypes. $^{**}p < 0.01$, $^{***}p < 0.001$ determined by one-way ANOVA and Holm-Sidak multiple comparison test. (C) Representative immunofluorescence images of the tumor core from day 8 SM1WT1 tumors grown in mice with the specified genotypes. Scale bars represent 100 μm.

Recent developments in understanding the positioning of immune cell infiltrate within the TME and how it influences prognosis (Fridman et al., 2012) led us to investigate $CD8^+$ T cell localization. We defined the tumor core versus invasive margin by intensity and nuclei density using DAPI staining as previously described (Figure S3B) (Lee et al., 2011). When comparing the ratio of $CD8^+$ infiltrate in the tumor core with invasive margin, the tumors in the DKO mice displayed a significantly higher such ratio compared with WT and CD73-deficient mice (Figure 2E). Preferential $CD8^+$ T cell distribution within the tumor core compared with the invasive margin has been shown to reflect a positive prognosis and improved therapeutic response in a number of cancers (Erdag et al., 2012; Halama et al., 2011; Tumeh et al., 2014). Therefore, loss of A2AR and CD73 may drive improved immune cell infiltration, particularly $CD8^+$ T cells, into the tumor core, explaining better tumor control. We next assessed whether $CD8^+$ T cells were functionally critical in the anti-tumor immune response against SM1WT1 primary tumors observed in DKO mice. Depletion of $CD8^+$ T cells resulted in loss of tumor control by DKO mice and single-gene-targeted mice (Figures 2F, 2G, and S3C–S3E).

Taken together, these data indicate that loss of A2AR signaling enhances immune cell infiltration, particularly of $CD8^+$ T cells, into the TME. Surprisingly, however, host CD73 deficiency did not appear to substantially change TIL infiltrate. Therefore, we aimed to identify the distinct role of CD73 in modulating the primary TME.

CD73 Is Upregulated on the Tumor and Host in A2AR-Deficient Mice

To identify the role of CD73 in the TME, we used immunofluorescence staining to assess CD73 co-localization with hematopoietic and non-hematopoietic cell types. Strikingly, we found that A2AR-deficient mice significantly upregulated CD73 expression within the core of the SM1WT1 tumors (Figures 3A–3C). Furthermore, CD73 upregulation in A2AR-deficient mice appeared to occur on both tumor and host, particularly endothelium (identified by CD31) (Figure 3C). WT mice displayed modest levels of CD73 expression, which often co-localized with endothelium. CD73.KO and DKO mice showed some tumor CD73 expression, which however was significantly lower than that observed in the A2AR-deficient mice (Figures 3B and 3C). Increased CD73 expression on both tumor and host in A2AR-deficient mice may represent a tumor escape mechanism, which is partially lost in DKO mice, unable to produce CD73 on host cells, indicating that this may contribute to the improved tumor control observed in these DKO mice.

Targeting A2AR and CD73 in Combination Improves Therapeutic Response

A2AR antagonism and antibody blockade of CD73 has been shown to enhance anti-tumor responses in a number of tumor models (Beavis et al., 2013; Stagg et al., 2010). Moreover, CD73 expression by the tumor appears to be necessary for eliciting maximal therapeutic benefit, indicating that CD73 may be a biomarker for stratifying patients toward therapies targeting the adenosinergic pathway (Beavis et al., 2013; Loi et al., 2013).

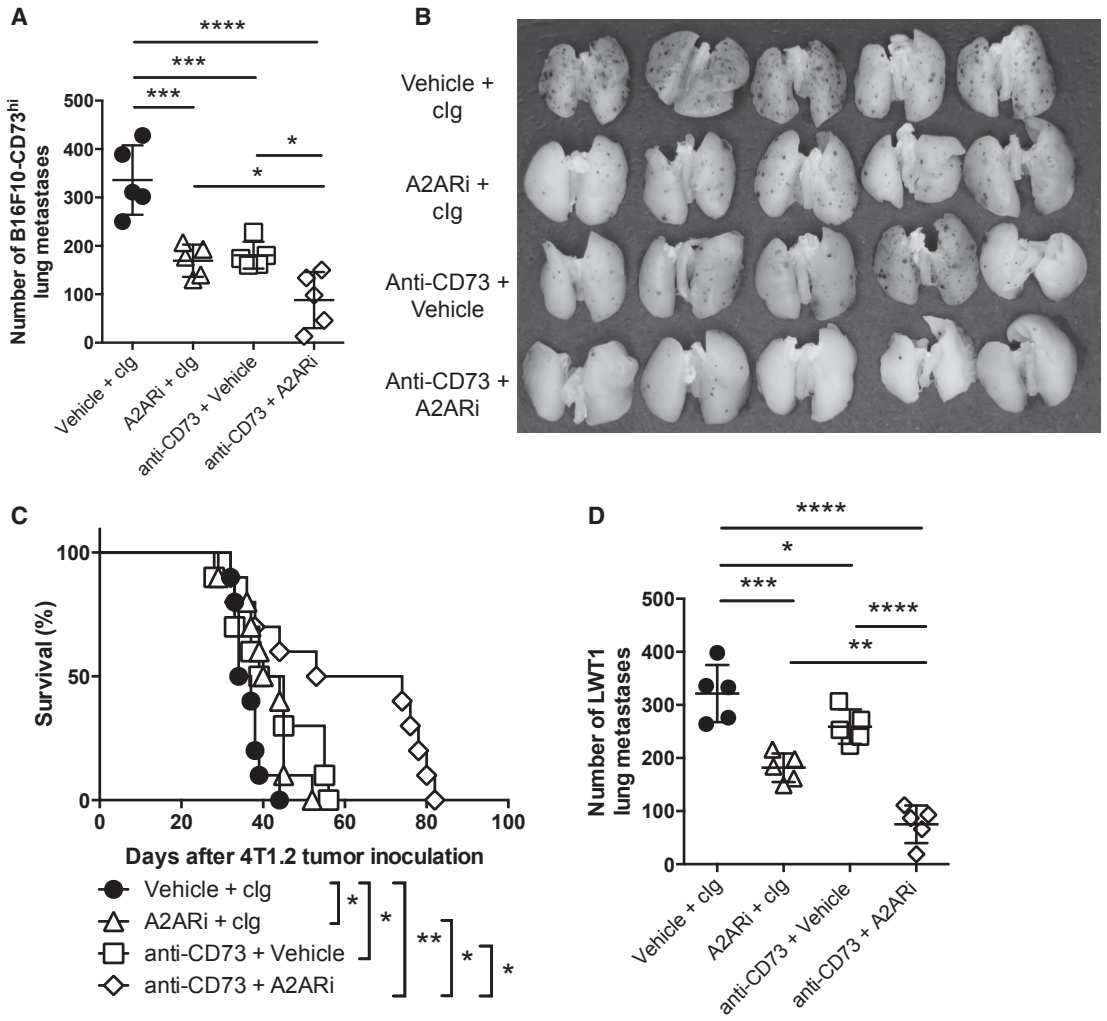

Figure 4. Anti-CD73 and A2ARi Suppress Experimental and Spontaneous Lung Metastasis

(A) Numbers of macrometastases in lungs harvested on day 14 from C57BL/6 WT mice injected intravenously with B16F10-CD73^{hi} and treated on days 0 and 3 intraperitoneally with vehicle, A2ARi (SCH58261, 1 mg/kg), clg (2A3, 250 μg), anti-CD73 (TY/23, 250 μg), or combinations as specified (n = 5 per group). Results are presented as mean ± SD from one representative experiment. *p < 0.05, ***p < 0.001, ****p < 0.0001 determined by one-way ANOVA and Holm-Sidak multiple comparison test.

(B) Metastatic burden of B16F10-CD73^{hi} tumor-bearing lungs at day 14 as in (A) from one representative experiment.

(C) Survival of female BALB/c WT mice injected in the mammary fat pad with 4T1.2, with the primary tumor resected on day 17 and treated intraperitoneally with vehicle, A2ARi (SCH58261, 1 mg/kg), clg (2A3, 250 μg), or anti-CD73 (TY/23, 250 μg) as indicated on days 18, 21, 24, and 27. *p < 0.05, **p < 0.01 determined by log-rank (Mantel-Cox) test.

(D) Numbers of macrometastases in lungs harvested on day 14 from male C57BL/6 WT mice injected intravenously with LWT1 and treated on days 0 and 3 intraperitoneally with vehicle, A2ARi (SCH58261, 1 mg/kg), clg (2A3, 250 μg), anti-CD73 (TY/23, 250 μg), or combinations as specified. Results are presented as mean ± SD from one experiment. *p < 0.05, **p < 0.01, ***p < 0.001, and ****p < 0.0001 determined by one-way ANOVA and Holm-Sidak multiple comparison test. See also Figure S4.

Therefore, we assessed the therapeutic efficacy of A2AR inhibitor (A2ARi) and anti-CD73 antibody in metastasis models known to be responsive to either monotherapy (Beavis et al., 2013; Stagg et al., 2010, 2011), namely the B16F10-CD73^{hi} experimental lung metastasis model and the 4T1.2 spontaneous metastasis model. We found that combining A2ARi (SCH58261) and anti-mouse CD73 antibody (TY/23) had better anti-metastatic efficacy compared with either monotherapy and control treatment (Figures 4A–4C). When given concurrently, these therapies significantly reduced the metastatic burden and enhanced survival (Figures 4A and 4C). In addition, we assessed this combination in the LWT1 experimental metastasis melanoma model that displayed reduced metastatic formation in DKO mice. While treatment with either A2ARi or anti-CD73 significantly decreased the metastatic burden compared with control treatment, the combination afforded significantly improved protection against metastasis (Figure 4D). Further investigation revealed that NK cells, CD8^{+} T cells, and interferon-γ (IFN-γ), and to a lesser extent perforin, were required for maximal combination activity (Figures S4A–S4D). Similarly,

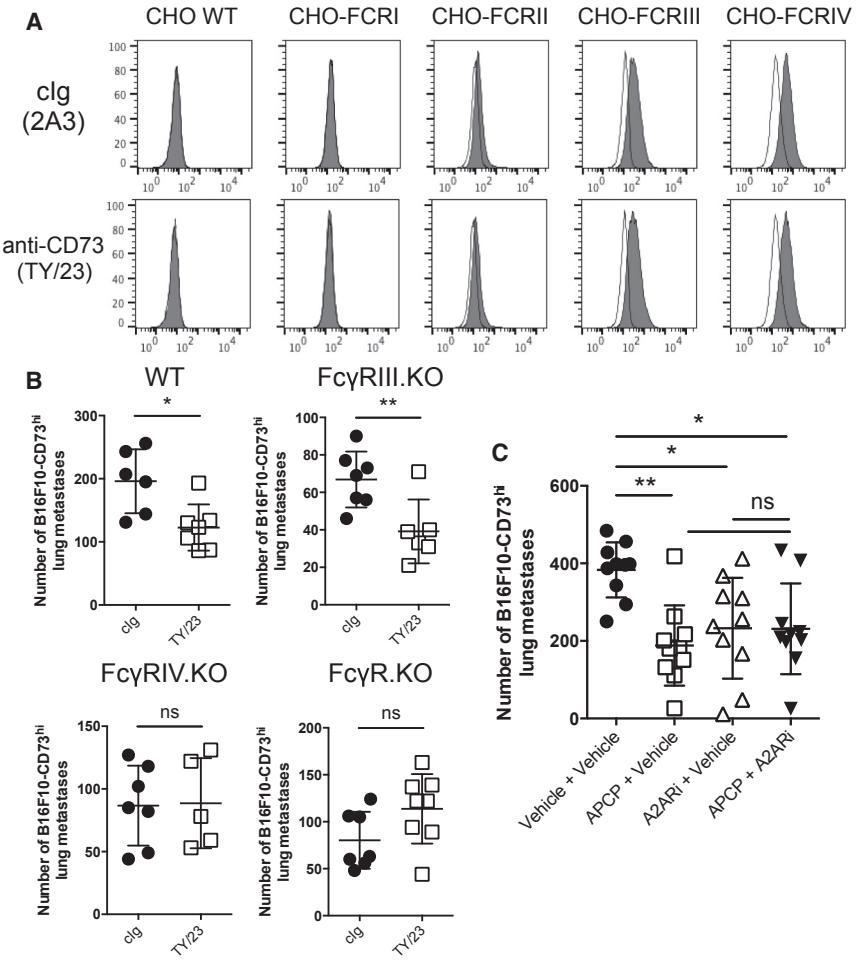

Figure 5. Anti-CD73 Requires Fc Receptor Engagement for Anti-metastatic Activity

(A) Binding of clg (2A3, 10 μg/mL) or anti-CD73 (TY/23, 10 μg/mL) to CHO cells ectopically expressing respective FLAG-tagged Fc receptor is shown as solid histograms. Unshaded histograms represent the binding of secondary goat anti-rat antibodies alone. The same secondary alone histogram is shown for both clg and anti-CD73 for an individual cell type.

(B) Numbers of macrometastases in lungs harvested on day 14 from C57BL/6 WT, FcγRIII.KO, FcγRIV.KO, and FcγR.KO (deficient for all activating Fc receptors) mice injected intravenously with B16F10-CD73^{hi} (10^5 cells or 5×10^4 cells for FcγR.KO mice) and treated intraperitoneally with clg (2A3, 250 μg) or TY/23 (250 μg) on days 0 and 3. Results are presented as mean ± SD from one representative experiment.

(C) Vehicle, APCP (400 μg), or A2ARi (1 mg/kg) were administered on day 0 and day 3 in the specified combinations. B16F10-CD73^{hi} tumor-bearing lungs were harvested on day 14 and macrometastases counted. Results are presented as mean ± SD from two pooled experiments of ten mice per treatment group.

*$p < 0.05$, **$p < 0.01$ determined by unpaired t test (B) or one-way ANOVA and Holm-Sidak multiple comparison test (C). ns, not significant. See also Figure S5.

anti-metastatic activity against LWT1 in DKO mice was mediated by NK cells (Figure S4E).

Anti-CD73 Requires Fc Receptor Engagement for Optimal Therapeutic Activity

While A2AR antagonism has primarily been attributed to enhancing lymphocyte-mediated anti-tumor immune responses (Beavis et al., 2013; Mittal et al., 2014), less is known regarding the mechanism of action by which anti-CD73 monoclonal antibody (mAb) elicits efficacy in vivo. Considering the impact of Fc receptor binding in providing optimal antibody activity (Dahan et al., 2015), we determined whether anti-mouse CD73 mAb required Fc receptor engagement for therapeutic activity. We first found that the rat anti-mouse CD73 mAb TY/23 was able to bind to mouse FcγRIII and FcγRIV activating receptors (Figures 5A and S5). We then compared the anti-metastatic activity of TY/23 in mice deficient for FcγRIII, FcγRIV, or all activating FcγR receptors. While both WT and FcγRIII-deficient mice had significantly reduced metastatic burden in response to TY/23 treatment, FcγRIV- or FcγR-deficient mice displayed no significant difference in metastasis formation compared with isotype control-treated mice (Figure 5B). Therefore, TY/23 is dependent at a minimum on host FcγRIV for optimal therapeutic activity. We then assessed whether blockade of CD73 adenosine generation, using the small molecule APCP, collaborated with inhibition of A2AR signaling to reduce metastasis. Interestingly, while each of A2AR and CD73 small-molecule inhibitors was able to decrease the number of metastases compared with vehicle controls, together they displayed no increased effect (Figure 5C). This illustrates that genetic or antibody-mediated loss of CD73 activity, by removal of CD73 on the cell surface or Fc receptor engagement, is required for improved therapeutic activity in the presence of A2AR antagonism. These data suggest a multi-functionality of CD73 as a target, beyond its ectonucleotidase activity.

CD11b$^+$Gr-1^{hi} Expansion Is Induced by Anti-CD73 Therapy

Next, given the anti-metastatic activity of anti-CD73 and dependence on FcγRIV, we assessed changes to the immune makeup of the pulmonary TME. We identified that the most prominent populations expressing FcγRIV in whole lung homogenates were the CD11b$^+$Gr-1^{hi} and CD11b$^+$Gr-1^{lo} myeloid cells (Figure 6A). Interestingly, following TY/23 therapy CD11b$^+$Gr-1^{hi} cells displayed an expansion in both proportion and number (Figure 6B). Further characterization of these cells revealed that they expressed high levels of Ly6G and low levels of F4/80, indicative of neutrophils (Figure S6A). Therefore, we investigated whether the CD11b$^+$Gr-1^{hi} cell expansion mediated anti-CD73 metastatic control (Figure S6B). Interestingly, following depletion of the CD11b$^+$Gr-1^{hi} cells by anti-Ly6G, TY/23 therapeutic efficacy was lost (Figure 6C).

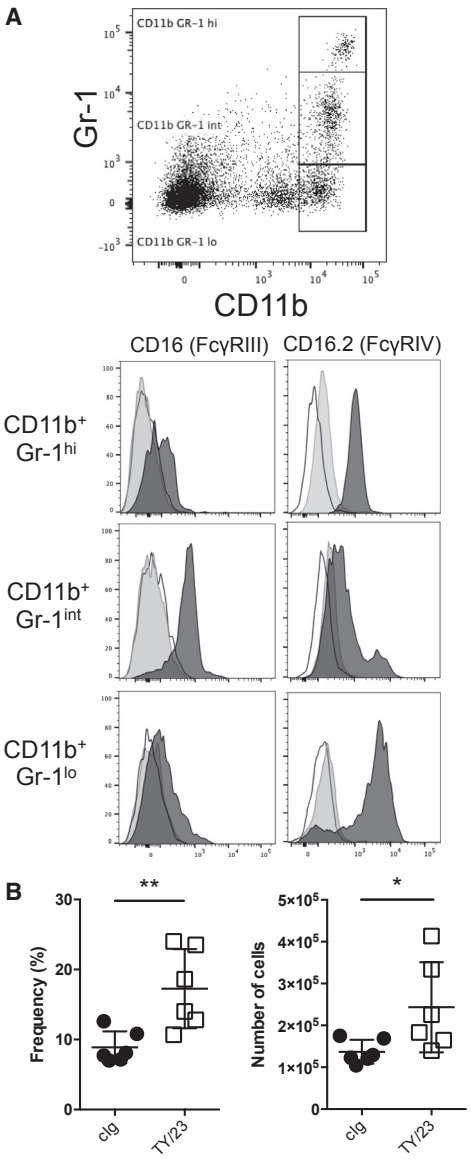

Figure 6. Expansion of CD11b$^+$Gr-1^{hi} Myeloid Cells in the Pulmonary Tumor Microenvironment Following Anti-CD73 Treatment

(A) Expression of CD16 (FcγRIII) or CD16.2 (FcγRIV) on different CD11b$^+$Gr-1 populations from lungs of WT mice was assessed by flow cytometry and shown as a representative black histogram. Unshaded histograms denote control isotype staining and gray histograms represent antibody staining in FcγRIII-deficient (left) or FcγRIV-deficient (right) mice.

(B) Groups of six C57BL/6 WT female mice were injected intravenously with B16F10-CD73^{hi} melanoma. On days 0 and 3, mice were treated intraperitoneally with clg (1-1, 250 μg) or TY/23 (250 μg). Tumor-bearing lungs were harvested on day 5, and frequency and number of CD11b$^+$Gr-1^{hi} cells determined by flow cytometry are shown as mean ± SD. *$p < 0.05$, **$p < 0.01$ determined by unpaired t test.

(C) C57BL/6 WT mice were injected intravenously with B16F10-CD73^{hi} melanoma. On days 0 and 3 after tumor inoculation, mice were treated intraperitoneally with clg (1-1, 250 μg) or TY/23 (250 μg). Some groups of mice received anti-Ly6G depletion (1A8, 500 μg intraperitoneally) on days −1 and 2. Lungs were harvested on day 14 and macrometastases counted. Results are presented as mean ± SD from one representative experiment of six to seven mice per treatment group. *$p < 0.05$ determined by one-way ANOVA and Holm-Sidak multiple comparison test.

(D) C57BL/6 WT and CD73.KO mice were injected intravenously with B16F10-CD73^{hi} melanoma. On days 0 and 3 after tumor inoculation, mice were treated intraperitoneally with clg (1-1, 250 μg) or TY/23 (250 μg). Lungs were harvested on day 14 and macrometastases counted. Results are presented as mean ± SD from two pooled experiments of ten mice per genotype and treatment group. *$p < 0.05$, ****$p < 0.0001$ determined by one-way ANOVA and Holm-Sidak multiple comparison test. See also Figure S6.

The CD11b$^+$Gr-1^{hi} cell population expresses high levels of both CD73 and FcγRIV (Figures 6A and S6C); therefore, we assessed whether the anti-metastatic activity of TY/23 was maintained in CD73-deficient mice following B16F10-CD73^{hi} inoculation. Notably, TY/23 therapeutic efficacy was observed in both the WT and CD73-deficient mice (Figure 6D). In addition, an increase in the frequency of CD11b$^+$Gr-1^{hi} cells was identified in the pulmonary TME of CD73.KO, but not FcγRIV.KO, mice following TY/23 therapy (Figure S6D). We then assessed whether TY/23 treatment affected metastasis of the parental B16F10 cells, which did not express CD73, and found that it did not (Figure S6E). Together, these data indicated that tumor-derived CD73 and FcγRIV on CD11b$^+$Gr-1^{hi} cells were essential for anti-CD73 therapeutic efficacy within the pulmonary TME.

Recent evidence from non-small cell lung cancer patients highlighted a potential role of tumor-associated neutrophils during early-stage human disease in enhancing NK cell and T cell activation via engagement of co-stimulatory molecules (Eruslanov et al., 2014). Therefore, we investigated whether the expression of co-stimulatory molecules such as CD80 and CD86 were modulated following anti-CD73 treatment. While there was no significant change in the frequency or intensity of these markers on CD11b$^+$Gr-1^{hi} cells following anti-CD73 treatment, the greater number and proportion within the lung microenvironment may further enhance a more permissive anti-tumor interaction (Figure S6F). In addition, CD73 expression on the CD11b$^+$Gr-1^{hi} population has been suggested to heighten their immunosuppressive functions, particularly via autocrine signaling through adenosine receptors (Ryzhov et al., 2011). Using a non-competing mAb for CD73 staining (Stagg et al., 2010), we were able to identify that CD73 was reduced on CD11b$^+$Gr-1^{hi} cells following TY/23 treatment, indicating that they may lose suppressive functions (Figure S6G). While other cell populations expressing high levels of CD73, CD4$^+$, and CD8$^+$ T cells displayed

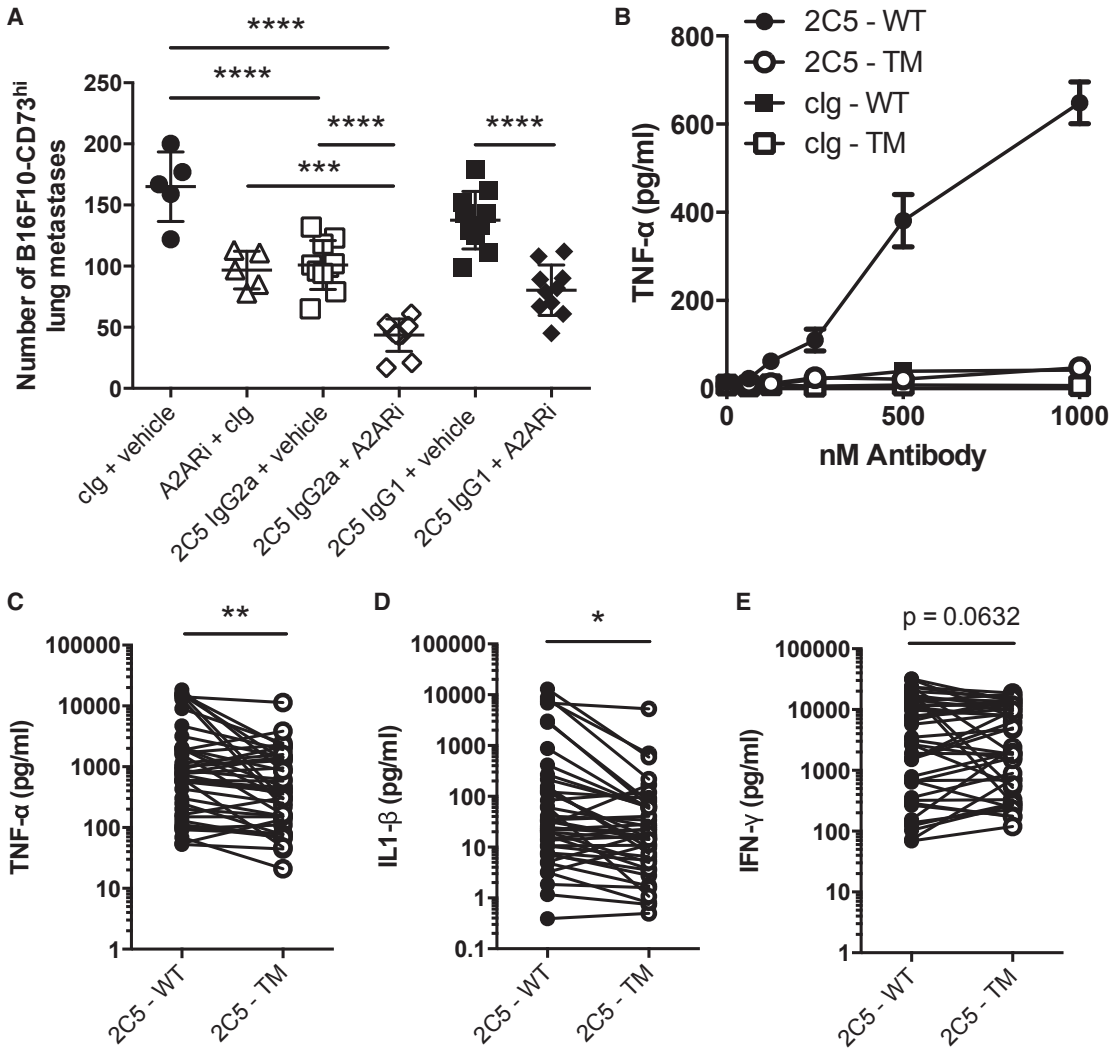

Figure 7. Human Anti-CD73 Requires Fc Receptor Engagement for Optimal Cytokine Production

(A) C57BL/6 WT mice were injected intravenously with B16F10-CD73^{hi} melanoma. On days 0 and 3, mice were treated intraperitoneally with vehicle, A2ARi (SCH58261, 1 mg/kg), clg (1-1, 250 μg), anti-CD73 (2C5 mouse IgG2a or 2C5 mouse IgG1, 250 μg) or combinations as specified. Lungs were harvested on day 14 and macrometastases counted and reported as mean ± SD. ***p < 0.001, ****p < 0.0001 determined by one-way ANOVA and Holm-Sidak multiple comparison test.

(B) Equal proportions of PBMC from two healthy donors were treated with increasing concentrations of human anti-CD73 (2C5 human IgG1 WT or triple mutant [TM]) or the appropriate isotype controls for 72 hr, and TNF-α levels in the supernatants were measured by ELISA (mean ± SD).

(C–E) Equal proportions of PBMC from 42 healthy donor pairs were treated with 1 μM of either human anti-CD73 (2C5 human IgG1 WT or 2C5 human IgG1 TM). After 72 hr, TNF-α (C), IL-1-β (D), and IFN-γ (E) levels in the supernatants were measured by ELISA. Statistical significance was determined by paired t test (*p < 0.05, **p < 0.01).

See also Figure S7.

no changes in proportions (Figure S6H), they similarly displayed a marked reduction in CD73 expression, which may result in reduced generation of adenosine within the tumor microenvironment (Figures S6I and S6J).

Human Anti-CD73 Enhances Cytokine Release by Fc Receptor Engagement

For both research and potential clinical uses we developed an anti-human CD73 mAb (clone 2C5) that is cross-reactive with mouse CD73. The specificity of 2C5 was validated by flow cytometry and its ability to inhibit CD73 ectonucleotidase activity (Figures S7A and S7B). We developed 2C5 with either a mouse immunoglobulin G2a (IgG2a) or IgG1 Fc region and assessed whether A2ARi was able to improve metastatic control in combination with them. Similarly to TY/23, 2C5 IgG2a provided significant protection against metastasis, which was enhanced in combination with A2ARi (Figure 7A). However, the 2C5 IgG1, which has limited Fc receptor binding capacity, displayed no significant metastatic control alone or in combination (Figure 7A).

Next, we assessed whether a fully human anti-CD73 was able to modulate cytokine production in a mixed leukocyte reaction (MLR) culture system. Notably, 2C5 with human IgG1, which

was able to interact with Fc receptors, enhanced tumor necrosis factor α (TNF-α) production (Figure 7B). However, when anti-CD73 was unable to bind Fc receptors, due to a triple mutation present within the human IgG1 backbone (Oganesyan et al., 2008), its ability to stimulate a cytokine response was reduced (Figure 7B). This was further validated by MLR using a number of donor-recipient pair combinations in which there was significantly higher TNF-α and interleukin 1β (IL-1β) production and a trend for higher levels of IFN-γ in the presence of WT anti-CD73 compared with the triple-mutated Fc receptor-impaired version of anti-CD73 (Figures 7C–7E). This is again indicative of the relationship between optimal anti-CD73 function and Fc receptor binding capability.

DISCUSSION

We have investigated whether the anti-tumor activity of combined inhibition of CD73 and A2AR is more potent than inhibition of either alone. Interestingly, rather than displaying redundancy, targeting these interdependent pathways in combination very significantly suppressed tumor initiation, growth, and metastasis. While the A2AR has been shown to mediate immunosuppression predominantly in immune cells from myeloid and lymphocyte lineages (Cekic et al., 2014; Cekic and Linden, 2014; Ohta et al., 2006), reducing adenosine signaling via A2AR antagonism provides an alternative targeted strategy to modulate the number and efficacy of infiltrating effector T cells within the immunosuppressive TME. Gene-targeting A2AR also illustrated the important role that host A2AR plays in regulating CD73 expression levels, particularly in the tumor. CD73 is a biomarker of poor prognosis for patients in a number of cancer types (Leclerc et al., 2016; Loi et al., 2013; Turcotte et al., 2015; Wu et al., 2012), but the role of CD73 as a therapeutic target is becoming increasingly complex. Alongside its ability to produce extracellular adenosine, CD73 has also been associated with modulating leukocyte and tumor migration and angiogenesis (Algars et al., 2011; Allard et al., 2014; Loi et al., 2013; Turcotte et al., 2015). We have highlighted the very important role activating Fc receptor (FcR) engagement might play in the activity of mAbs targeting mouse and human CD73. These are critical findings given that both CD73 and A2AR antagonists will play an increasingly important part in combination immunotherapies that include immune checkpoint inhibitors and conventional therapies that initiate immunogenic cell death (Beavis et al., 2015; Iannone et al., 2014; Loi et al., 2013; Mittal et al., 2014).

From the recent development of FDA-approved immunotherapies targeting immune checkpoint inhibitors, it is clear that patients may be stratified for their clinical response based on features present within the TME (Teng et al., 2015). For instance, anti-PD-1 therapeutic efficacy in metastatic melanoma appears optimal in a TME with a high presence of TILs and PD-L1 expression. Development and clinical translation of adenosine-related therapies will require effective selection of cancer subtypes and stratification of patients in order to recognize their therapeutic potential. In preclinical studies, expression of CD73 by tumor cells appears necessary for effective therapeutic activity of A2AR antagonists either alone or in combination (Beavis et al., 2013; Loi et al., 2013; Mittal et al., 2014). Therefore, assessing the CD73 status of patient tumors prior to therapy may be helpful in identifying those likely to respond to A2AR inhibition. Here we show the superior anti-metastatic activity of anti-CD73 against B16F10-CD73^{hi} tumors compared with parental CD73^{-} B16F10 tumors, and the activity of anti-CD73 in CD73-deficient mice. Yet, it is important to note that there may be tumors in which tumor cells fail to express CD73 but CD73 expression in the TME is sufficient for anti-CD73 mAb efficacy (eg. anti-CD73 against CT26; Hay et al., Abstract 285. AACR Meeting, Philadelphia, April 18-22, 2015). In addition, the role of CD73 in the TME appears to be diverse and may not be detrimental to the patient in all cancer cases. Recent studies in endometrial cancer identified that CD73 downregulation reduces cellular adhesion, correlating with increased clinical staging and reduced survival (Bowser et al., 2016). Understanding whether CD73 status on tumor cells or in the TME is predictive of clinical outcome will be an important factor in defining the suitability of different tumor types for treatment by adenosine-targeted therapies.

While CD73 within the TME has different functions, determining processes that modulate CD73 expression remains unclear. Hypoxia and ischemia play an important role in heightening the release of extracellular ATP that is subsequently converted to adenosine by CD73 (Young et al., 2014). However, hypoxia may also directly alter CD73 levels and the amount of CD39, the enzyme that converts ATP to AMP within the TME, thus further enhancing adenosine accumulation. Transcriptional activation of both CD73 and CD39 appears regulated by the hypoxia-inducible transcription factor HIF-1α (Synnestvedt et al., 2002). Similarly, in response to respiratory hyperoxia, T regulatory cells within the pulmonary TME decrease both CD73 and CD39 expression, impeding adenosine generation and promoting tumor control (Hatfield et al., 2014). In addition, conditional deletion of TGF-β signaling specifically on myeloid cells results in downregulation of CD73 and CD39 on infiltrating myeloid cells within the TME (Ryzhov et al., 2014). The protumorigenic signaling molecule TGF-β has been shown to stabilize HIF-1α (McMahon et al., 2006), indicative of interrelated mechanisms that may heighten CD73 expression. In our study, we identified that loss of host A2AR signaling increased CD73 expression within the tumor core. However, this appears to be reliant initially on the ability for the host, rather than tumor cells, to initiate an increase in CD73 levels, since host-deficiency of both A2AR and CD73 restricted changes to CD73 expression in the tumor core. Therefore, insufficient adenosine signaling within the TME may drive a feedback loop via induction of CD73 in order to increase adenosine levels in an attempt to resolve immune homeostasis and dampen immune activation. This provides important considerations for A2AR antagonists, and indeed alternate adenosine-related therapies, as they progress to clinical utility. Examining the interaction and modulation of the CD73-adenosinergic pathway in response to therapeutic intervention and tumor development will provide improved insight into the regulation and requirement of this molecule within a cancer setting.

The development of distinct immunomodulatory mAbs has generated much interest in the treatment of cancer. However, mAbs exert their effects through the Fab region and the Fc domain. Dependent on the Fc domain, recognition by immune cells can promote alternate mechanisms of action including

antibody-dependent cellular cytotoxicity and antibody-dependent cellular phagocytosis. Consideration of the Fc interaction within the TME appears necessary to improve mAb activity and limit toxicity. In particular, CTLA-4 is prominently expressed on T regulatory cells infiltrating into the TME. Through Fcγ receptor engagement, anti-CTLA-4 mAb exerts part of its effect in mice by initiating the depletion of this suppressive cell type, potently enhancing anti-tumor immune activity (Simpson et al., 2013). Preclinical development of agonistic antibodies against GITR and OX40 similarly identified that Fcγ receptor engagement was required to alter the intratumoral effector/regulatory T cell ratio, critical for therapeutic response (Bulliard et al., 2013, 2014). In contrast, anti-PD-1 mAb, reactive with an alternate immune checkpoint molecule, is not only Fc-independent, but when engineered to engage activating Fcγ receptors its therapeutic activity is abrogated (Dahan et al., 2015). In the same study, it was found that mAbs directed toward the PD-1 ligand, PD-L1, utilized Fcγ receptor binding to modulate the proportion of different subsets of myeloid cells within the tumor, resulting in improved tumor control (Dahan et al., 2015). The variation in mAb requirement of FcR engagement and its ability to modulate therapeutic activity indicates that this should always be assessed prior to clinical utility. However, whether FcR engagement is critical for optimal mAb activity in humans is less clear, with no strong evidence supporting a role for FcR in the clinical activity of ipilimumab (IgG1) or tremelimumab, which is IgG2 with little or no FcR engagement. Investigating the interactions between anti-CD73 and Fc engagement we identified that the Fc/FcR was contributing to cytokine stimulation and therapeutic activity. While we report an alternate function of TY/23 that utilizes FcγRIV, our study and others have shown that CD73 generation of adenosine is inhibited by APCP, and this inhibition is sufficient to promote anti-tumor activity (Iannone et al., 2014; Stagg et al., 2011; Wang et al., 2011). An important consideration is whether this is tumor microenvironment dependent. In addition, TY/23 has also been shown to block CD73 enzymatic activity and initiate CD73 internalization (Stagg et al., 2010). Our studies illustrate the importance of the host FcR in the anti-metastatic mechanism of action of TY/23, but also indicate some down modulation of CD73 on intratumor T cells after TY/23 administration. Recently, a human IgG2-IgG1 hybrid anti-human CD73 mAb lacking Fc function with internalization properties was described where durable reduction of surface CD73 was an important mechanism (Barnhart et al., Abstract 1476. AACR Meeting, New Orleans, April 15-20, 2016). Collectively, these findings have important implications for the development of anti-CD73 mAb therapies.

CD73 is widely expressed on both hematopoietic and non-hematopoietic cell types therefore Fcγ receptor engagement poses a potential toxicity risk (Young et al., 2014). Consistent with this concern, the first anti-CD73 antibody in clinical trials, MEDI9447, was engineered to reduce FcR engagement (Oganesyan et al., 2008). That said, it is interesting that no overt signs of toxicity have been identified using several different anti-CD73 mAbs in preclinical studies. Anti-CD73 may be an optimal candidate for utilization in a bispecific antibody approach to overcome systemic toxicity (Kontermann, 2012). Co-targeting anti-CD73, which limits immunosuppression, angiogenesis, and tumor cell migration and metastasis, using a tumor-specific marker to localize the bispecific therapy to the TME, may initiate tumor control and limit peripheral damage.

Therapeutic interventions targeting the adenosinergic pathway prevent tumor escape and tumor-derived immunosuppression in preclinical studies. In this study we demonstrated that co-targeting A2AR antagonism and CD73, via antibody-directed therapies that engage Fcγ receptors, is an effective combinatorial approach. As A2AR inhibitors and anti-CD73 mAbs progress to oncology use, these findings should have broad implications for clinical regimens and approaches to adenosine-related treatment.

EXPERIMENTAL PROCEDURES

Mice

C57BL/6 and BALB/c WT mice were purchased from the Walter and Eliza Hall Institute for Medical Research or bred in-house at the QIMR Berghofer Medical Research Institute. C57BL/6 FcR-deficient (FcγR.KO, FcγRIII.KO, and FcγRIV.KO) (kindly provided by Mark Hogarth and Jeffrey Ravetch, respectively) (Giorgini et al., 2008; Hazenbos et al., 1996; Nimmerjahn et al., 2010; Takai et al., 1994), and C57BL/6 A2AR-deficient (A2AR.KO) (Beavis et al., 2013; Chen et al., 1999) and CD73-deficient (CD73.KO) (Stagg et al., 2011; Thompson et al., 2004) mice were as described. C57BL/6 A2AR.CD73-deficient (DKO) mice were derived by crossing A2AR.KO and CD73.KO mice at the QIMR Berghofer Medical Research Institute. WT and all gene-targeted strains were used between the ages of and 20 weeks. Groups of 5–23 mice per experiment were used for experimental tumor assays to ensure adequate power to detect biological differences. All experiments were approved by the QIMR Berghofer Medical Research Institute Animal Ethics Committee.

Tumor Cell Lines

The C57BL/6 SM1WT1, LWT1, and B16F10-CD73^{hi} melanoma, AT-3 mammary adenocarcinoma, RMA-s-luciferase^{+} T lymphoma, and BALB/c 4T1.2 were maintained as previously described (Beavis et al., 2013; Ferrari de Andrade et al., 2014; Ngiow et al., 2011; Souza-Fonseca-Guimaraes et al., 2015; Verbrugge et al., 2012). B16F10-CD73^{hi} and AT-3 were grown in DMEM (Gibco) supplemented with 10% fetal calf serum (FCS), 1% Glutamax (Gibco), and 1% penicillin/streptomycin (Gibco) maintained at 5% and 10% CO_2, respectively. 4T1.2, SM1WT1, LWT1, and RMA-s-luciferase^{+} cells were grown in RPMI 1640 (Gibco) supplemented with 10% FCS, 1% Glutamax (Gibco), and 1% penicillin/streptomycin (Gibco) and maintained at 5% CO_2.

Antibodies and Reagents

Purified anti-mouse CD73 mAb (clones TY/23 and 2C5), control Ig (clones 2A3, 1-1, and 1A7), anti-CD8β (53-5.8), and anti-Ly6G (1A8) were purchased from BioXCell or supplied by Medimmune, and administered at the schedule and dose as indicated. SCH58621 was purchased from Sigma and used at 1 mg/kg intraperitoneally per dose. Anti-CD73 antibody 2C5 was discovered and optimized for CD73 binding and neutralization using established phage display methodology. The 2C5-TM (triple mutant) form of the antibody encodes a triple mutation in the constant region of the heavy chain to reduce IgG effector function (Oganesyan et al., 2008).

In Vivo Treatments

For primary tumor growth experiments, 10^6 SM1WT1 or AT-3 tumor cells were subcutaneously injected into mice in a volume of 100 μL (day 0). Tumor growth was measured using digital calipers, and tumor sizes represented. At indicated time points, tumors were excised and mass (in mg) measured for individual mice in each group. For spontaneous metastasis following surgical resection survival experiments, 2×10^4 or 5×10^4 4T1.2 tumor cells were injected orthotopically into the fourth mammary fat pad of BALB/c strain mice. On days 16–20, while mice were anesthetized, the primary tumor was surgically removed and the wound closed with surgical clips, and post-surgery treatment commenced as indicated. Survival was measured, and mice were euthanized according to ethical endpoints and autopsied to confirm formation of metastases. For experimental metastasis, 10^5 or 5×10^4 B16F10-CD73^{hi}, or 5×10^4

RMA-s-luciferase$^+$, or 5 × 10^5 LWT1 cells were injected intravenously in a 200-μL volume into selected strains of mice and treatment commenced immediately after (day 0) and on day 3, as indicated. Mice injected with RMA-s-luciferase$^+$ T lymphoma were followed for survival and euthanized according to ethically approved endpoints. Lungs of B16F10-CD73^{hi} and LWT1 tumor-bearing mice were harvested on day 14 and macrometastases on the lung surface counted using a dissecting microscope.

MCA-Induced Fibrosarcoma

For MCA carcinogen-induced fibrosarcoma formation, groups of 19–23 male WT, A2AR.KO, CD73.KO, or DKO mice were injected subcutaneously on the right flank with 300 μg of MCA and monitored over 200 days for fibrosarcoma development. Data were recorded as the percentage of tumor-free mice in which tumors were recorded following two consecutive growth measurements.

Flow Cytometry Analysis

Tumors, tumor-bearing lungs, peripheral lymphoid tissues, and blood were harvested from naive mice from various genotypes and therapeutically treated mice, as indicated. Tumors and lungs were minced and digested with 1 mg/mL collagenase IV (Worthington Biochemical) and 0.02 mg/mL DNaseI (Roche) and homogenized to prepare single cell suspensions. Spleens were homogenized and red blood cells (RBCs) lysed in preparation for flow cytometry. Similarly, RBCs from peripheral blood samples were lysed twice in preparation for flow cytometry. For surface staining, TIL or immune cell suspensions were stained with eFluor780 anti-CD45.2 (104; eBioscience), Brilliant Violet 605 anti-CD4 (RM4-5; Biolegend), APC anti-CD8α (53-6.7; Biolegend), fluorescein isothiocyanate (FITC) and PercpCy5.5 anti-TCRβ (H57-597; Biolegend), phycoerythrin (PE) and BV605 anti-CD11b (M1/70; eBioscience and Biolegend), eFluor450 anti-Gr-1 (RB6-8C5; eBioscience), PE-Cy7 anti-NK1.1 (PK136; eBioscience), PE-Cy7 and PE anti-F4/80 (BM8; Biolegend), PE anti-CD73 (TY/23; BD Bioscience), PE-Cy7 anti-CD73 (TY/11.8; eBioscience), APC anti-mouse CD16 (FcγRIII), and purified anti-mouse CD16.2 (FcγRIV) (9E9; Biolegend) followed by FITC goat anti-hamster (Armenian), IgG FITC goat anti-hamster (Armenian), IgG (Poly4055; Biolegend), and respective isotype antibodies in the presence of anti-CD16/32 (2.4G2) unless otherwise indicated. 7AAD or Zombie Aqua (Biolegend) was used to exclude dead cells. Cells were acquired on the BD LSR II Fortessa (BD Biosciences) and analysis was carried out using FlowJo (Tree Star).

Immunohistochemistry

Tumors were excised on day 8 and freshly frozen in optimal cutting temperature compound. Frozen sections were cut from the tumors and fixed in cold 100% acetone. Sections were blocked with Background Sniper (Biocare), then stained with FITC anti-CD8α (53-6.7; eBioscience), APC anti-CD31 (MEC 13.3; BD Bioscience), and PE anti-CD73 (TY/23; BD Bioscience). Tiled images of the whole tumor section were captured on a Zeiss 780 laser scanning confocal microscope on a 20× objective (numerical aperture 0.8). Analysis was performed using Imaris (Bitplane). Tumor boundary and margin boundary were identified by a minimum of two independent reviewers to calculate area of tumor. Numbers of CD8$^+$ cells within the tumor versus margin were automatically detected in Imaris and normalized to region area. Mean fluorescence intensity of CD73 was determined using MATLAB (MathWorks).

Fc Receptor Binding Assay

CHO cells transfected with FLAG-tagged murine Fc receptors (Mancardi et al., 2008) were cultured in DMEM, 1% Glutamax (Gibco), and 1% penicillin/streptomycin (Gibco), non-essential amino acids, and sodium pyruvate as well as specific selection media including 1 mg/mL geneticin and 0.5 mg/mL zeocin as required. At 90% confluence the cells were seeded at 2 × 10^5 cells and incubated with 10 μg/mL anti-CD73 (TY/23) or cIg (2A3) as specified. Cells were then washed and a secondary goat anti-rat IgG conjugated to AlexaFluor 488 (Poly4054; Biolegend) was used to detect specific Fc receptor bound antibody by flow cytometry.

Mixed Leukocyte Reaction

Peripheral blood mononuclear cells (PBMCs) were isolated fresh from healthy donors or from frozen healthy Leukopak aliquots. For fresh PBMCs, blood from healthy donors was collected into 8-mL BD Vacutainer CPT cell preparation tubes and then centrifuged for 20 min at 2,700 rpm. PBMCs were collected and washed three times with AIM-V assay medium (Gibco). RBCs were lysed using RBC Lysing Buffer (Gibco). PBMCs were prepared from Leukopaks (All Cells) by collection into 1-L bottles and dilution with wash buffer (PBS containing 2% fetal bovine serum). PBMCs were then isolated by layering over LSM Separation Medium (MP Biomedicals) in 50-mL Sepmate tubes (Stem Cell Technologies). Cells were collected following centrifugation at 1,200 × *g* for 10 min and then washed by centrifugation three times with wash buffer at 300 × *g* for 8 min. RBCs were lysed using RBC Lysing Buffer (Gibco). PBMCs were resuspended in Cell Freezing Medium (Gibco) and frozen at −80°C. For the MLR, PBMCs were resuspended in assay medium. PBMCs from two donors were mixed together in a 1:1 ratio within AIM-V medium and plated into 96-well U-bottomed plates (Costar) at a density of 2 × 10^5 cells per well per donor in 100 μL of medium. 2C5 and an isotype control antibody were diluted in serum-free AIM-V medium and then added to the cells for 72–96 hr. Plates were then centrifuged at 1,500 rpm for 3 min. Supernatant was harvested and then assayed for cytokine secretion using the human TH1/TH2 multiplex ELISA (Meso Scale Discovery) according to the manufacturer's instructions. Healthy donors supplying PBMCs were anonymously enrolled in the MedImmune Research Specimen Collection Program. Individuals with HIV infection, hepatitis B or C virus, human T-lymphotropic virus, or syphilis were excluded. All protocols and informed consent forms were approved by Chesapeake Institutional Review Board and all donors provided signed consent.

Statistics

Statistical analyses were carried out using GraphPad Prism software. Significant differences were determined by log-rank t test and ANOVA, and Holm-Sidak multiple comparison test of all pairwise combinations between genotypes were determined unless indicated, with unpaired and paired t test as specified. Values of $p < 0.05$ were considered significant.

SUPPLEMENTAL INFORMATION

Supplemental Information includes Supplemental Experimental Procedures and seven figures and can be found with this article online at http://dx.doi.org/10.1016/j.ccell.2016.06.025.

AUTHOR CONTRIBUTIONS

Conceptualization, A.Y., K.S., and M.J.S.; Methodology, A.Y., S.F.N., D.S.B., K.S., and M.J.S.; Investigation, A.Y., S.F.N., D.S.B., S.J.B., E.S., C.H., Q.H., J.L., and M.J.S.; Resources, K.T. and K.S.; Funding Acquisition, M.J.S. and M.W.L.T.; Writing – Original Draft, A.Y. and M.J.S.; Writing – Review & Editing, A.Y., S.F.N., S.J.B., K.S., and M.J.S.; Visualization, A.Y., D.S.B., and M.J.S.; Supervision, A.Y., K.S., M.W.L.T., and M.J.S.

ACKNOWLEDGMENTS

The authors wish to thank Liam Town, Kate Elder, and Joanne Sutton for maintaining the mice used in this study. We thank the QIMR Berghofer Medical Research Institute flow cytometry and imaging facilities, particularly Tam Nguyen and Nigel Waterhouse for assistance with acquiring data. We thank Jeffrey Ravetch and Mark Hogarth for providing the original C57BL/6 FcγRIII, FcγRIV, and FcγR gene-targeted breeding pairs. We thank Pierre Bruhns for providing the Fc receptor transfected CHO cells. M.J.S. was supported by a National Health and Medical Research Council of Australia (NHMRC) Senior Research Fellowship (1078671), a Susan G. Komen Program Grant (IIR12221504), and a Cancer Research Institute Clinical Strategy Team Grant. A.Y. was supported by a Cancer Council Queensland Ph.D. fellowship. S.F.N was supported by an NHMRC C.J. Martin Fellowship (1111469). M.J.S. has a research agreement with Bristol Myers Squibb and Medimmune. E.S., C.H., and K.S. are employees of Medimmune.

Received: February 25, 2016
Revised: June 7, 2016
Accepted: August 5, 2016
Published: September 12, 2016

REFERENCES

Algars, A., Karikoski, M., Yegutkin, G.G., Stoitzner, P., Niemela, J., Salmi, M., and Jalkanen, S. (2011). Different role of CD73 in leukocyte trafficking via blood and lymph vessels. Blood *117*, 4387–4393.

Allard, B., Pommey, S., Smyth, M.J., and Stagg, J. (2013). Targeting CD73 enhances the antitumor activity of anti-PD-1 and anti-CTLA-4 mAbs. Clin. Cancer Res. *19*, 5626–5635.

Allard, B., Turcotte, M., Spring, K., Pommey, S., Royal, I., and Stagg, J. (2014). Anti-CD73 therapy impairs tumor angiogenesis. Int. J. Cancer *134*, 1466–1473.

Beavis, P.A., Divisekera, U., Paget, C., Chow, M.T., John, L.B., Devaud, C., Dwyer, K., Stagg, J., Smyth, M.J., and Darcy, P.K. (2013). Blockade of A2A receptors potently suppresses the metastasis of CD73+ tumors. Proc. Natl. Acad. Sci. USA *110*, 14711–14716.

Beavis, P.A., Milenkovski, N., Henderson, M.A., John, L.B., Allard, B., Loi, S., Kershaw, M.H., Stagg, J., and Darcy, P.K. (2015). Adenosine receptor 2A blockade increases the efficacy of anti-PD-1 through enhanced antitumor T-cell responses. Cancer Immunol. Res. *3*, 506–517.

Bowser, J.L., Blackburn, M.R., Shipley, G.L., Molina, J.G., Dunner, K., Jr., and Broaddus, R.R. (2016). Loss of CD73-mediated actin polymerization promotes endometrial tumor progression. J. Clin. Invest. *126*, 220–238.

Bulliard, Y., Jolicoeur, R., Windman, M., Rue, S.M., Ettenberg, S., Knee, D.A., Wilson, N.S., Dranoff, G., and Brogdon, J.L. (2013). Activating Fc gamma receptors contribute to the antitumor activities of immunoregulatory receptor-targeting antibodies. J. Exp. Med. *210*, 1685–1693.

Bulliard, Y., Jolicoeur, R., Zhang, J., Dranoff, G., Wilson, N.S., and Brogdon, J.L. (2014). OX40 engagement depletes intratumoral Tregs via activating FcgammaRs, leading to antitumor efficacy. Immunol. Cell Biol. *92*, 475–480.

Cekic, C., and Linden, J. (2014). Adenosine A2A receptors intrinsically regulate CD8+ T cells in the tumor microenvironment. Cancer Res. *74*, 7239–7249.

Cekic, C., Day, Y.J., Sag, D., and Linden, J. (2014). Myeloid expression of adenosine A2A receptor suppresses T and NK cell responses in the solid tumor microenvironment. Cancer Res. *74*, 7250–7259.

Chen, J.F., Huang, Z., Ma, J., Zhu, J., Moratalla, R., Standaert, D., Moskowitz, M.A., Fink, J.S., and Schwarzschild, M.A. (1999). A(2A) adenosine receptor deficiency attenuates brain injury induced by transient focal ischemia in mice. J. Neurosci. *19*, 9192–9200.

Dahan, R., Sega, E., Engelhardt, J., Selby, M., Korman, A.J., and Ravetch, J.V. (2015). FcgammaRs modulate the anti-tumor activity of antibodies targeting the PD-1/PD-L1 axis. Cancer Cell *28*, 285–295.

Eini, H., Frishman, V., Yulzari, R., Kachko, L., Lewis, E.C., Chaimovitz, C., and Douvdevani, A. (2015). Caffeine promotes anti-tumor immune response during tumor initiation: involvement of the adenosine A2A receptor. Biochem. Pharmacol. *98*, 110–118.

Erdag, G., Schaefer, J.T., Smolkin, M.E., Deacon, D.H., Shea, S.M., Dengel, L.T., Patterson, J.W., and Slingluff, C.L., Jr. (2012). Immunotype and immunohistologic characteristics of tumor-infiltrating immune cells are associated with clinical outcome in metastatic melanoma. Cancer Res. *72*, 1070–1080.

Eruslanov, E.B., Bhojnagarwala, P.S., Quatromoni, J.G., Stephen, T.L., Ranganathan, A., Deshpande, C., Akimova, T., Vachani, A., Litzky, L., Hancock, W.W., et al. (2014). Tumor-associated neutrophils stimulate T cell responses in early-stage human lung cancer. J. Clin. Invest. *124*, 5466–5480.

Ferrari de Andrade, L., Ngiow, S.F., Stannard, K., Rusakiewicz, S., Kalimutho, M., Khanna, K.K., Tey, S.K., Takeda, K., Zitvogel, L., Martinet, L., and Smyth, M.J. (2014). Natural killer cells are essential for the ability of BRAF inhibitors to control BRAFV600E-mutant metastatic melanoma. Cancer Res. *74*, 7298–7308.

Fridman, W.H., Pages, F., Sautes-Fridman, C., and Galon, J. (2012). The immune contexture in human tumours: impact on clinical outcome. Nat. Rev. Cancer *12*, 298–306.

Giorgini, A., Brown, H.J., Lock, H.R., Nimmerjahn, F., Ravetch, J.V., Verbeek, J.S., Sacks, S.H., and Robson, M.G. (2008). FcγRIII and FcγRIV are indispensable for acute glomerular inflammation induced by switch variant monoclonal antibodies. J. Immunol. *181*, 8745–8752.

Halama, N., Michel, S., Kloor, M., Zoernig, I., Benner, A., Spille, A., Pommerencke, T., von Knebel, D.M., Folprecht, G., Luber, B., et al. (2011). Localization and density of immune cells in the invasive margin of human colorectal cancer liver metastases are prognostic for response to chemotherapy. Cancer Res. *71*, 5670–5677.

Hatfield, S.M., Kjaergaard, J., Lukashev, D., Belikoff, B., Schreiber, T.H., Sethumadhavan, S., Abbott, R., Philbrook, P., Thayer, M., Shujia, D., et al. (2014). Systemic oxygenation weakens the hypoxia and hypoxia inducible factor 1alpha-dependent and extracellular adenosine-mediated tumor protection. J. Mol. Med. *92*, 1283–1292.

Hatfield, S.M., Kjaergaard, J., Lukashev, D., Schreiber, T.H., Belikoff, B., Abbott, R., Sethumadhavan, S., Philbrook, P., Ko, K., Cannici, R., et al. (2015). Immunological mechanisms of the antitumor effects of supplemental oxygenation. Sci. Transl. Med. *7*, 277ra230.

Hazenbos, W.L., Gessner, J.E., Hofhuis, F.M., Kuipers, H., Meyer, D., Heijnen, I.A., Schmidt, R.E., Sandor, M., Capel, P.J., Daeron, M., et al. (1996). Impaired IgG-dependent anaphylaxis and Arthus reaction in Fc gamma RIII (CD16) deficient mice. Immunity *5*, 181–188.

Iannone, R., Miele, L., Maiolino, P., Pinto, A., and Morello, S. (2014). Adenosine limits the therapeutic effectiveness of anti-CTLA4 mAb in a mouse melanoma model. Am. J. Cancer Res. *4*, 172–181.

Knight, D.A., Ngiow, S.F., Li, M., Parmenter, T., Mok, S., Cass, A., Haynes, N.M., Kinross, K., Yagita, H., Koya, R.C., et al. (2013). Host immunity contributes to the anti-melanoma activity of BRAF inhibitors. J. Clin. Invest. *123*, 1371–1381.

Kontermann, R.E. (2012). Dual targeting strategies with bispecific antibodies. MAbs *4*, 182–197.

Leclerc, B.G., Charlebois, R., Chouinard, G., Allard, B., Pommey, S., Saad, F., and Stagg, J. (2016). CD73 expression is an independent prognostic factor in prostate cancer. Clin. Cancer Res. *22*, 158–166.

Lee, J., Borboa, A.K., Baird, A., and Eliceiri, B.P. (2011). Non-invasive quantification of brain tumor-induced astrogliosis. BMC Neurosci. *12*, 9.

Loi, S., Pommey, S., Haibe-Kains, B., Beavis, P.A., Darcy, P.K., Smyth, M.J., and Stagg, J. (2013). CD73 promotes anthracycline resistance and poor prognosis in triple negative breast cancer. Proc. Natl. Acad. Sci. USA *110*, 11091–11096.

Mancardi, D.A., Iannascoli, B., Hoos, S., England, P., Daeron, M., and Bruhns, P. (2008). FcgammaRIV is a mouse IgE receptor that resembles macrophage FcepsilonRI in humans and promotes IgE-induced lung inflammation. J. Clin. Invest. *118*, 3738–3750.

McMahon, S., Charbonneau, M., Grandmont, S., Richard, D.E., and Dubois, C.M. (2006). Transforming growth factor beta1 induces hypoxia-inducible factor-1 stabilization through selective inhibition of PHD2 expression. J. Biol. Chem. *281*, 24171–24181.

Mittal, D., Young, A., Stannard, K., Yong, M., Teng, M.W., Allard, B., Stagg, J., and Smyth, M.J. (2014). Antimetastatic effects of blocking PD-1 and the adenosine A2A receptor. Cancer Res. *74*, 3652–3658.

Ngiow, S.F., von Scheidt, B., Akiba, H., Yagita, H., Teng, M.W.L., and Smyth, M.J. (2011). Anti-TIM3 antibody promotes T cell IFN-γ-mediated antitumor immunity and suppresses established tumors. Cancer Res. *71*, 3540–3551.

Ngiow, S.F., Young, A., Jacquelot, N., Yamazaki, T., Enot, D., Zitvogel, L., and Smyth, M.J. (2015). A threshold level of intratumor CD8+ T-cell PD1 expression dictates therapeutic response to anti-PD1. Cancer Res. *75*, 3800–3811.

Nimmerjahn, F., Lux, A., Albert, H., Woigk, M., Lehmann, C., Dudziak, D., Smith, P., and Ravetch, J.V. (2010). FcγRIV deletion reveals its central role for IgG2a and IgG2b activity in vivo. Proc. Natl. Acad. Sci. USA *107*, 19396–19401.

Oganesyan, V., Gao, C., Shirinian, L., Wu, H., and Dall'Acqua, W.F. (2008). Structural characterization of a human Fc fragment engineered for lack of effector functions. Acta Crystallogr. D Biol. Crystallogr. *64*, 700–704.

Ohta, A., and Sitkovsky, M. (2001). Role of G-protein-coupled adenosine receptors in downregulation of inflammation and protection from tissue damage. Nature *414*, 916–920.

Ohta, A., Gorelik, E., Prasad, S.J., Ronchese, F., Lukashev, D., Wong, M.K., Huang, X., Caldwell, S., Liu, K., Smith, P., et al. (2006). A2A adenosine receptor protects tumors from antitumor T cells. Proc. Natl. Acad. Sci. USA *103*, 13132–13137.

Ott, P.A., Hodi, F.S., and Robert, C. (2013). CTLA-4 and PD-1/PD-L1 blockade: new immunotherapeutic modalities with durable clinical benefit in melanoma patients. Clin. Cancer Res. *19*, 5300–5309.

Ryzhov, S., Novitskiy, S.V., Goldstein, A.E., Biktasova, A., Blackburn, M.R., Biaggioni, I., Dikov, M.M., and Feoktistov, I. (2011). Adenosinergic regulation of the expansion and immunosuppressive activity of CD11b+Gr1+ cells. J. Immunol. *187*, 6120–6129.

Ryzhov, S.V., Pickup, M.W., Chytil, A., Gorska, A.E., Zhang, Q., Owens, P., Feoktistov, I., Moses, H.L., and Novitskiy, S.V. (2014). Role of TGF-beta signaling in generation of CD39+CD73+ myeloid cells in tumors. J. Immunol. *193*, 3155–3164.

Simpson, T.R., Li, F., Montalvo-Ortiz, W., Sepulveda, M.A., Bergerhoff, K., Arce, F., Roddie, C., Henry, J.Y., Yagita, H., Wolchok, J.D., et al. (2013). Fc-dependent depletion of tumor-infiltrating regulatory T cells co-defines the efficacy of anti-CTLA-4 therapy against melanoma. J. Exp. Med. *210*, 1695–1710.

Smyth, M.J., Ngiow, S.F., Ribas, A., and Teng, M.W. (2015). Combination cancer immunotherapies tailored to the tumour microenvironment. Nat. Rev. Clin. Oncol. *13*, 143–158.

Souza-Fonseca-Guimaraes, F., Young, A., Mittal, D., Martinet, L., Bruedigam, C., Takeda, K., Andoniou, C.E., Degli-Esposti, M.A., Hill, G.R., and Smyth, M.J. (2015). NK cells require IL-28R for optimal in vivo activity. Proc. Natl. Acad. Sci. USA *112*, E2376–E2384.

Stagg, J., Divisekera, U., McLaughlin, N., Sharkey, J., Pommey, S., Denoyer, D., Dwyer, K.M., and Smyth, M.J. (2010). Anti-CD73 antibody therapy inhibits breast tumor growth and metastasis. Proc. Natl. Acad. Sci. USA *107*, 1547–1552.

Stagg, J., Divisekera, U., Duret, H., Sparwasser, T., Teng, M.W., Darcy, P.K., and Smyth, M.J. (2011). CD73-deficient mice have increased antitumor immunity and are resistant to experimental metastasis. Cancer Res. *71*, 2892–2900.

Stagg, J., Beavis, P.A., Divisekera, U., Liu, M.C., Moller, A., Darcy, P.K., and Smyth, M.J. (2012). CD73-deficient mice are resistant to carcinogenesis. Cancer Res. *72*, 2190–2196.

Swann, J.B., Hayakawa, Y., Zerafa, N., Sheehan, K.C., Scott, B., Schreiber, R.D., Hertzog, P., and Smyth, M.J. (2007). Type I IFN contributes to NK cell homeostasis, activation, and antitumor function. J. Immunol. *178*, 7540–7549.

Synnestvedt, K., Furuta, G.T., Comerford, K.M., Louis, N., Karhausen, J., Eltzschig, H.K., Hansen, K.R., Thompson, L.F., and Colgan, S.P. (2002). Ecto-5'-nucleotidase (CD73) regulation by hypoxia-inducible factor-1 mediates permeability changes in intestinal epithelia. J. Clin. Invest. *110*, 993–1002.

Takai, T., Li, M., Sylvestre, D., Clynes, R., and Ravetch, J.V. (1994). FcR gamma chain deletion results in pleiotrophic effector cell defects. Cell *76*, 519–529.

Teng, M.W., Ngiow, S.F., Ribas, A., and Smyth, M.J. (2015). Classifying cancers based on t-cell infiltration and PD-L1. Cancer Res. *75*, 2139–2145.

Thompson, L.F., Eltzschig, H.K., Ibla, J.C., Van De Wiele, C.J., Resta, R., Morote-Garcia, J.C., and Colgan, S.P. (2004). Crucial role for ecto-5'-nucleotidase (CD73) in vascular leakage during hypoxia. J. Exp. Med. *200*, 1395–1405.

Tumeh, P.C., Harview, C.L., Yearley, J.H., Shintaku, I.P., Taylor, E.J., Robert, L., Chmielowski, B., Spasic, M., Henry, G., Ciobanu, V., et al. (2014). PD-1 blockade induces responses by inhibiting adaptive immune resistance. Nature *515*, 568–571.

Turcotte, M., Spring, K., Pommey, S., Chouinard, G., Cousineau, I., George, J., Chen, G.M., Gendoo, D.M., Haibe-Kains, B., Karn, T., et al. (2015). CD73 is associated with poor prognosis in high-grade serous ovarian cancer. Cancer Res. *75*, 4494–4503.

Verbrugge, I., Hagekyriakou, J., Sharp, L.L., Galli, M., West, A., McLaughlin, N.M., Duret, H., Yagita, H., Johnstone, R.W., Smyth, M.J., and Haynes, N.M. (2012). Radiotherapy increases the permissiveness of established mammary tumors to rejection by immunomodulatory antibodies. Cancer Res. *72*, 3163–3174.

Wang, L., Fan, J., Thompson, L.F., Zhang, Y., Shin, T., Curiel, T.J., and Zhang, B. (2011). CD73 has distinct roles in nonhematopoietic and hematopoietic cells to promote tumor growth in mice. J. Clin. Invest. *121*, 2371–2382.

Wu, X.R., He, X.S., Chen, Y.F., Yuan, R.X., Zeng, Y., Lian, L., Zou, Y.F., Lan, N., Wu, X.J., and Lan, P. (2012). High expression of CD73 as a poor prognostic biomarker in human colorectal cancer. J. Surg. Oncol. *106*, 130–137.

Young, A., Mittal, D., Stagg, J., and Smyth, M.J. (2014). Targeting cancer-derived adenosine: new therapeutic approaches. Cancer Discov. *4*, 879–888.